Supporting Information

Porous Organic Polymers Containing Active Metal Centers for Suzuki-Miyaura Heterocoupling Reactions

Noelia Esteban[1], María L. Ferrer[2], Conchi O. Ania[3], José G. de la Campa[4], Ángel E. Lozano[1,4,5], Cristina Álvarez[4,5,], Jesús A. Miguel[1,*]*

1. IU CINQUIMA, Universidad de Valladolid, Paseo Belén 5, E-47011 Valladolid, Spain.

2. Materials Science Factory, Instituto de Ciencia de Materiales de Madrid, ICMM-CSIC, Campus de Cantoblanco, 28049 Madrid, Spain.

3. CEMHTI CNRS (UPR 3079), University of Orléans, 45071 Orléans, France.

4. Department of Applied Macromolecular Chemistry, Instituto de Ciencia y Tecnología de Polímeros, ICTP-CSIC, Juan de la Cierva 3, E-28006 Madrid, Spain.

5. SMAP, UA-UVA_CSIC, Associated Research Unit to CSIC. Universidad de Valladolid, Facultad de Ciencias, Paseo Belén 7, E-47011 Valladolid, Spain.

Corresponding authors; Cristina Álvarez, cristina.alvarez@ictp.csic.es and Jesús A. Miguel, jamiguel@uva.es

CONTENTS

Section 1. Synthesis and characterization of 4,5-diazafluoren-9-one (DAFO)

Materials

1, 10-Phenantroline (+99%), isatin (1H-indol-2,3-dione; 98%), 1,3,5-triphenylbenzene (+99%), 4-bromoanisole y 4-bromotoluene were purchased from AlfaAesar. Anhydrous chloroform and 4-chlorotoluene were bought from Acros Organics. $NaHCO_3$ was acquired from Panreac. 1-bromonaphtalene and 1-bromo-4-*tert*-butylbenzene were bought from Aldrich. 1,3-dibromo-5-*tert*-butyl-benzene was purchased from ABCR. Triflic acid and phenylboronic acid were acquired from FluoroChem. 4-Metoxyphenyl boronic acid was purchased from Apollo Scientific. Na_2CO_3 was bought from Merck. Ethanol was acquired from Scharlau. Dichloromethane was purchased from Carlo Erba, and palladium(II) acetate was acquired from Johnson Matthey.

Synthesis of 4,5-diazafluoren-9-one

4,5-diazafluoren-9-one (DAFO) was synthesized following the methodology described elsewhere [31,32]. Following the Scheme 1, in a first step, a mixture (2:1) of H_2SO_4 (125 mL) and HNO_3 (63 mL) was carefully added to a mixture of 1,10-phenantroline (12.4 g, 68.9 mmol) and KBr (12.8 g, 108 mmol) on an ice bath. The reaction was left to reflux for 3 h and then neutralized and washed twice with an aqueous solution of NaOH. The product 1,10-phenantroline-5,6-dione (PHADO) was obtained with a 70% yield. The chemical structure of PHADO was confirmed by ^{1}H-NMR (Figure S1). Next, in a second step, PHADO (4.00 g, 19.0 mmol) was put to react with 0.25 M NaOH solution (200 mL) at 100 °C in an open flask until the volume was halved. Afterwards, the product was filtered, washed several times with distilled water and dried at 50ºC under vacuum. Finally, the DAFO was purified by filtration through aluminium oxide, using chloroform as solvent, and obtained in 81% yield (overall yield of 56%). The chemical structure of DAFO was confirmed by ^{1}H-RMN (Figure S2).

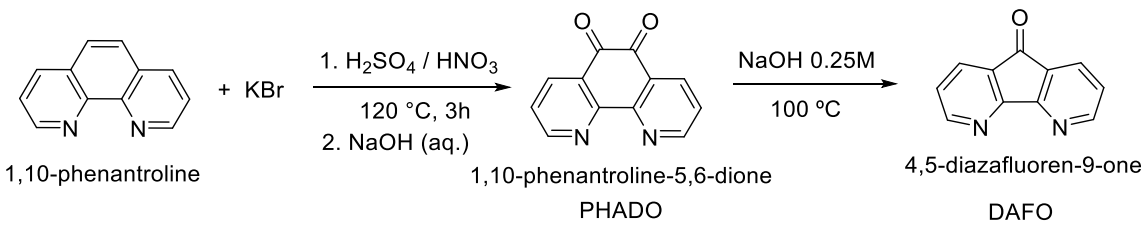

Scheme S1. Synthesis of DAFO

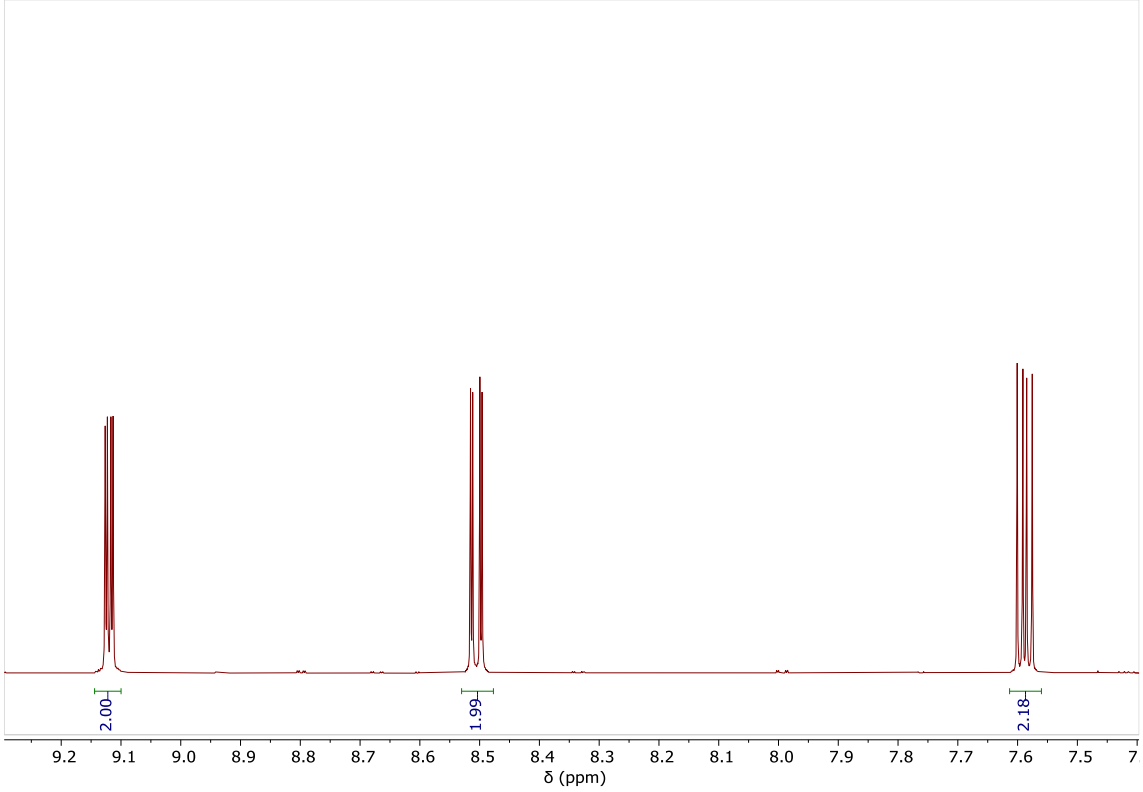

Figure S1. ^{1}H-NMR spectrum of PHADO (500 MHz, $CDCl_3$); δ (ppm): 9.12 (dd, J = 4.7, 1.8 Hz, 2H), 8.51 (dd, J = 7.8, 1.8 Hz, 2H), 7.59 (dd, J = 7.9, 4.7 Hz, 2H).

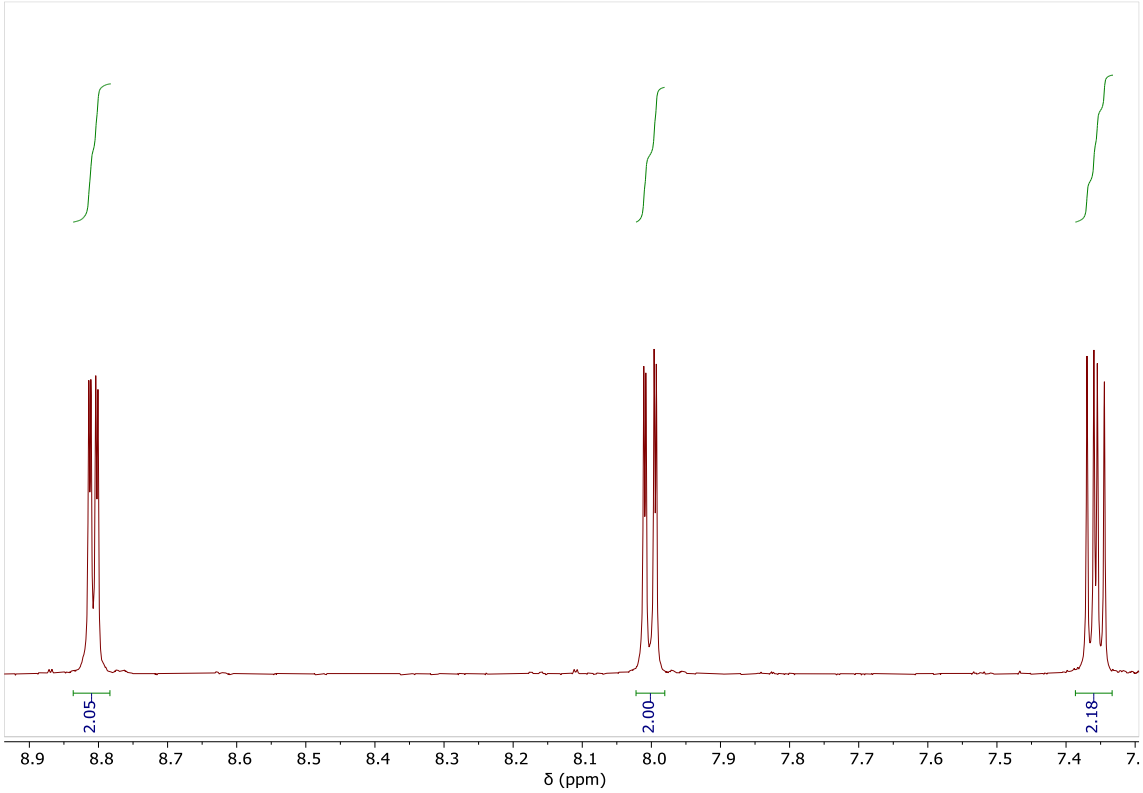

Figure S2. ^{1}H-NMR spectrum of DAFO (500 MHz, $CDCl_3$); δ(ppm): 8.81 (dd, J = 5.0, 1.6 Hz, 2H), 8.00 (dd, J = 7.5, 1.6 Hz, 2H), 7.36 (dd, J = 7.5, 5.0 Hz, 2H).

Section 2. Synthesis of porous organic polymers. Optimization of reaction conditions

Table S1. Synthesis conditions of POPs and yield.

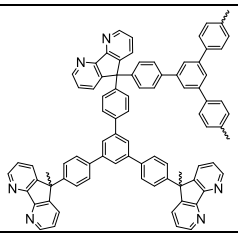				
135TPB-DAFO	time/temperature	TFSA	$CHCl_3$	Yield (%)
POP1-RT	120 h/RT	✓		92
POP1-60	24 h/RT, 96 h/60 ºC	✓		93
POP1-60/$CHCl_3$. **SP-POP1**	24 h/RT, 96 h/60 ºC	✓	✓	99
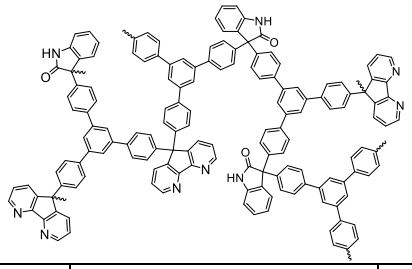				
135TPB-DAFO-isatin (4:3:3)	time/temperature	TFSA	$CHCl_3$	Yield (%)
POP2-60	24 h/RT, 96 h/60 ºC	✓		93
POP2-60/$CHCl_3$. **SP-POP2**	24 h/RT, 96 h/60 ºC	✓	✓	99
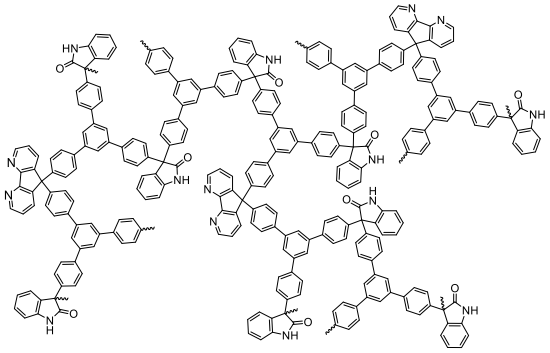				
135TPB-DAFO-isatin (8:3:9)	time/temperature	TFSA	$CHCl_3$	Yield (%)
POP3-RT	120 h/RT	✓	✓	99
POP3-60	24 h/RT, 96 h/60 ºC	✓		62
POP3-60/$CHCl_3$. **SP-POP3**	24 h/RT, 96 h/60 ºC	✓	✓	99
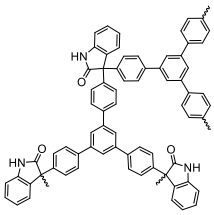				
135TPB-isatin	time/temperature	TFSA	$CHCl_3$	Yield (%)
POP4-RT/$CHCl_3$	120 h/RT	✓	✓	99

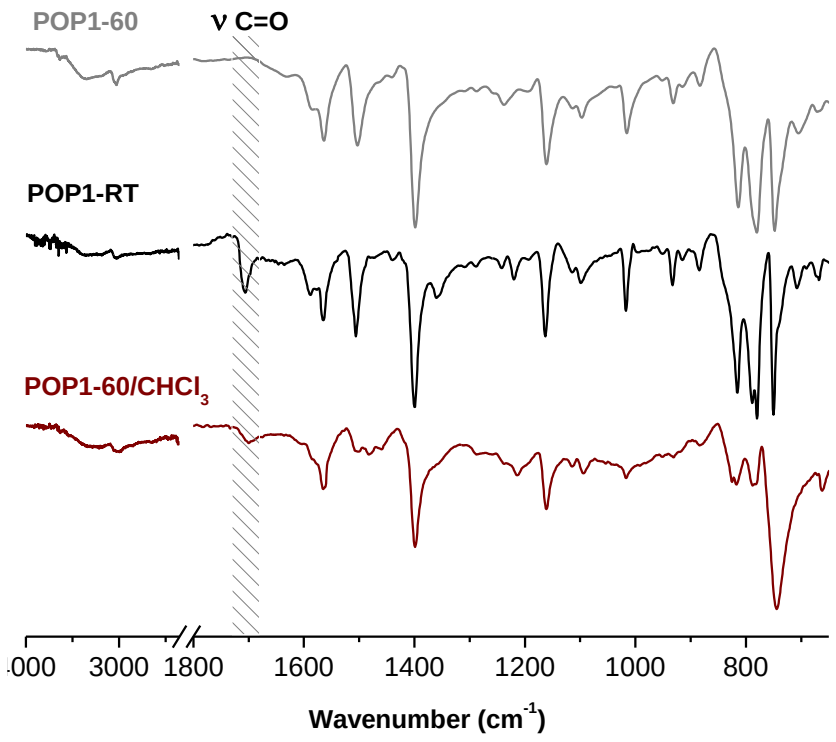

Figure S3. FTIR-ATR spectra of POP1 obtained using different reaction conditions. The dashed line region indicates the position of the C=O stretching coming from DAFO.

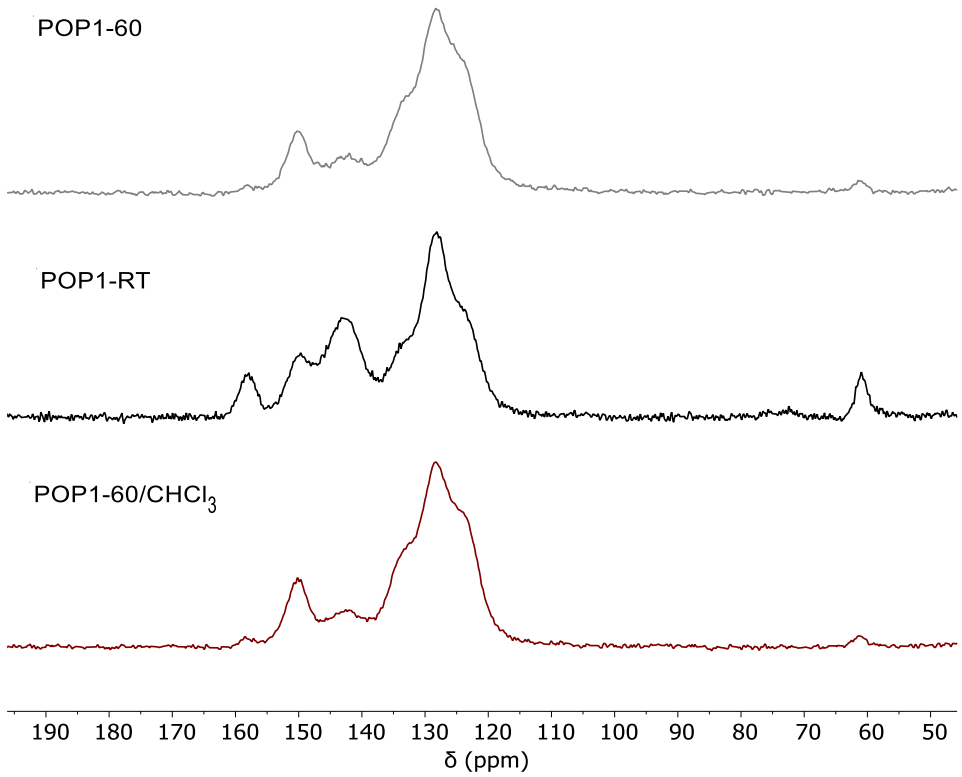

Figure S4. CP/MAS ^{13}C-NMR spectra of POP1 obtained using different reaction conditions.

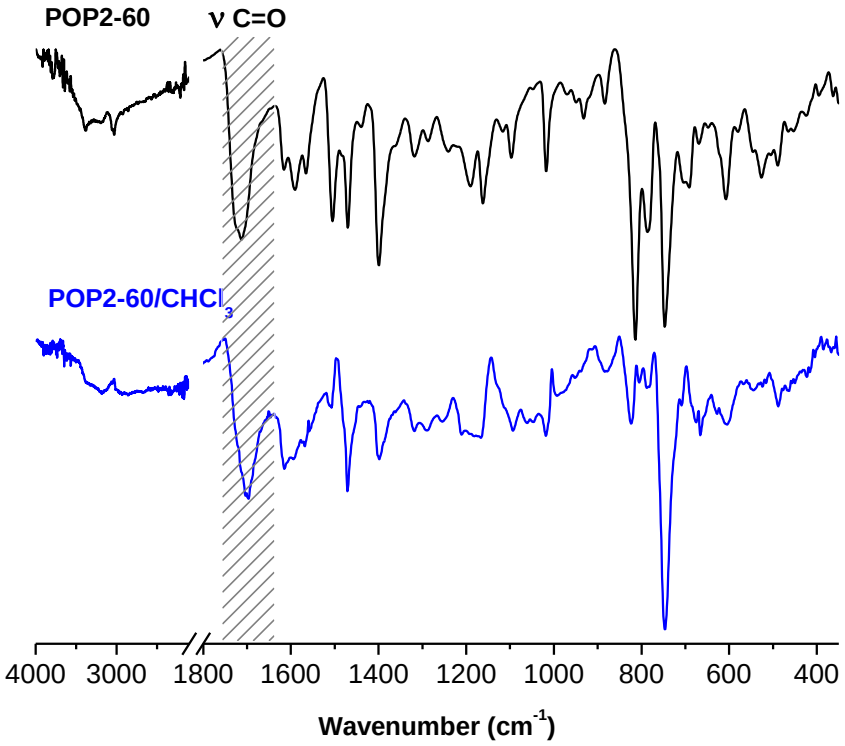

Figure S5. FTIR-ATR spectra of POP2 obtained using different reaction conditions. The dashed line region indicates the position of the C=O stretching coming from DAFO and from lactam ring formed during the reaction.

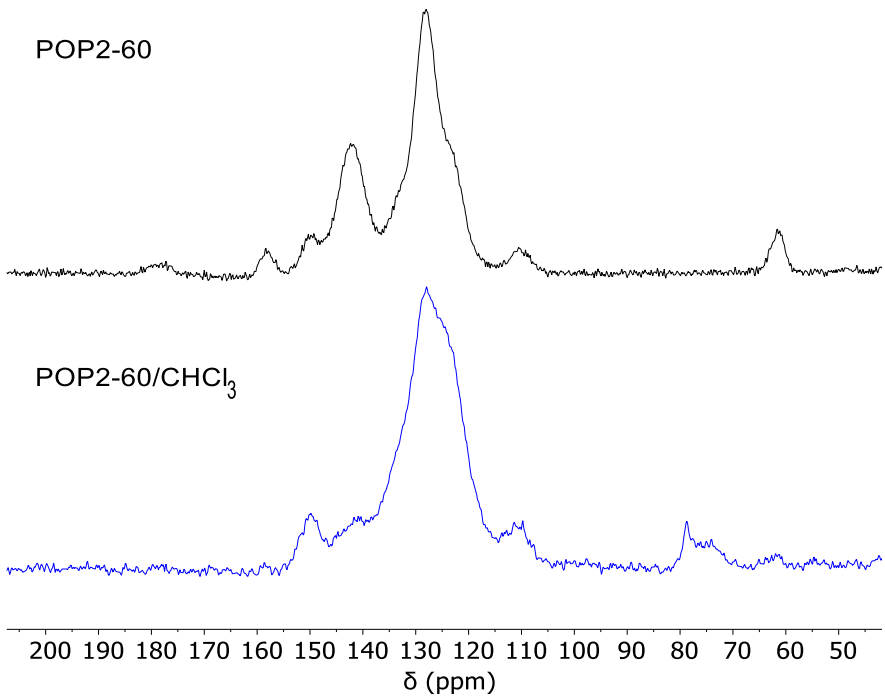

Figure S6. CP/MAS ^{13}C-NMR spectra of POP2 obtained using different reaction conditions.

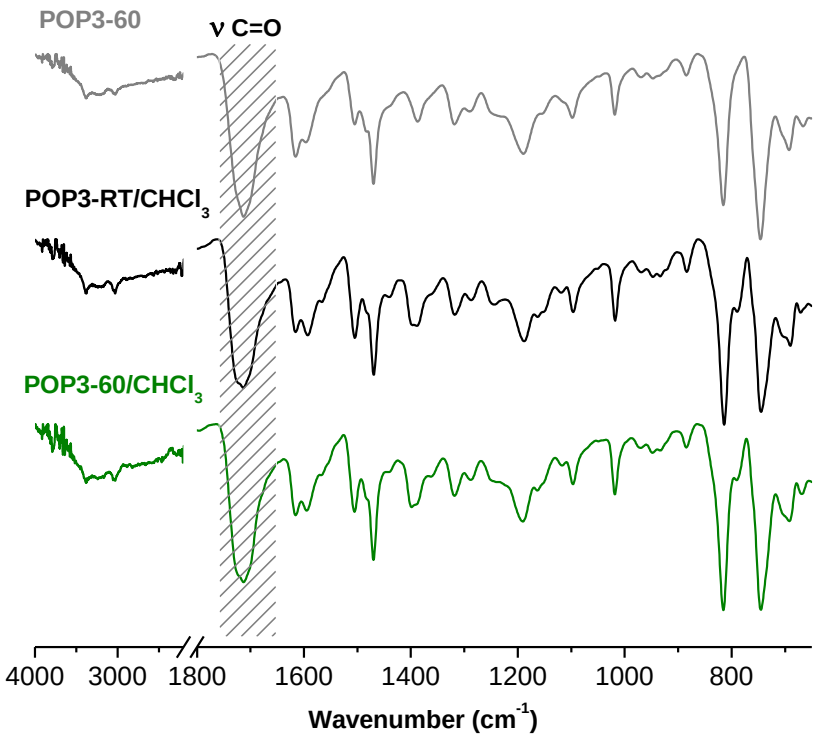

Figure S7. FTIR-ATR spectra of POP3 obtained by different reaction conditions. The dashed line region indicates the position of the C=O stretching coming from DAFO and from lactam ring formed during the reaction.

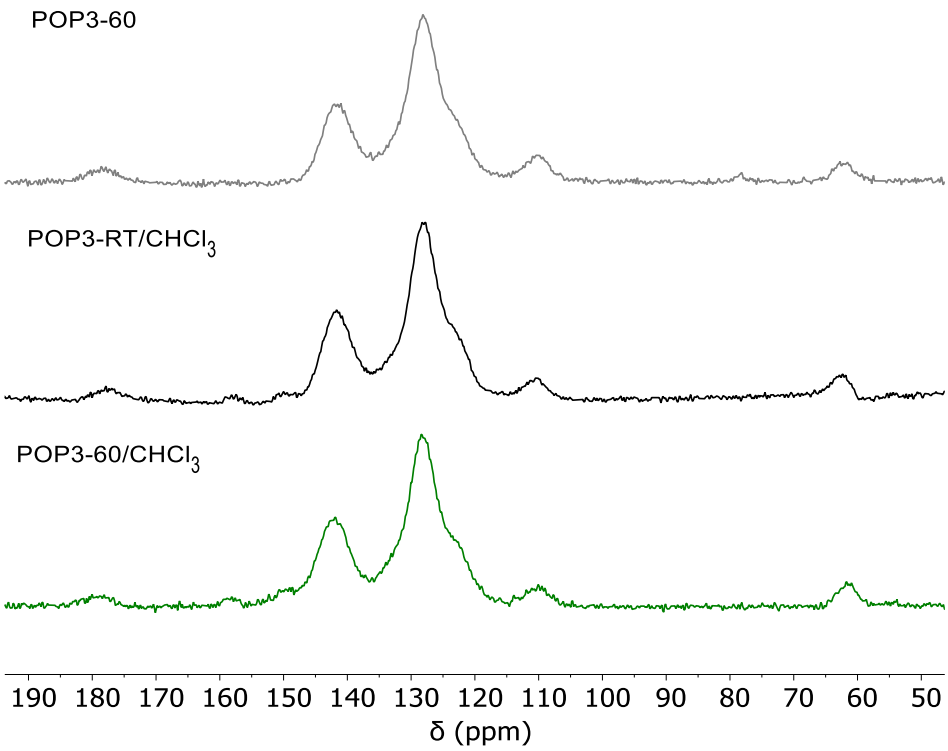

Figure S8. CP/MAS ^{13}C-NMR spectra of POP3 obtained using different reaction conditions.

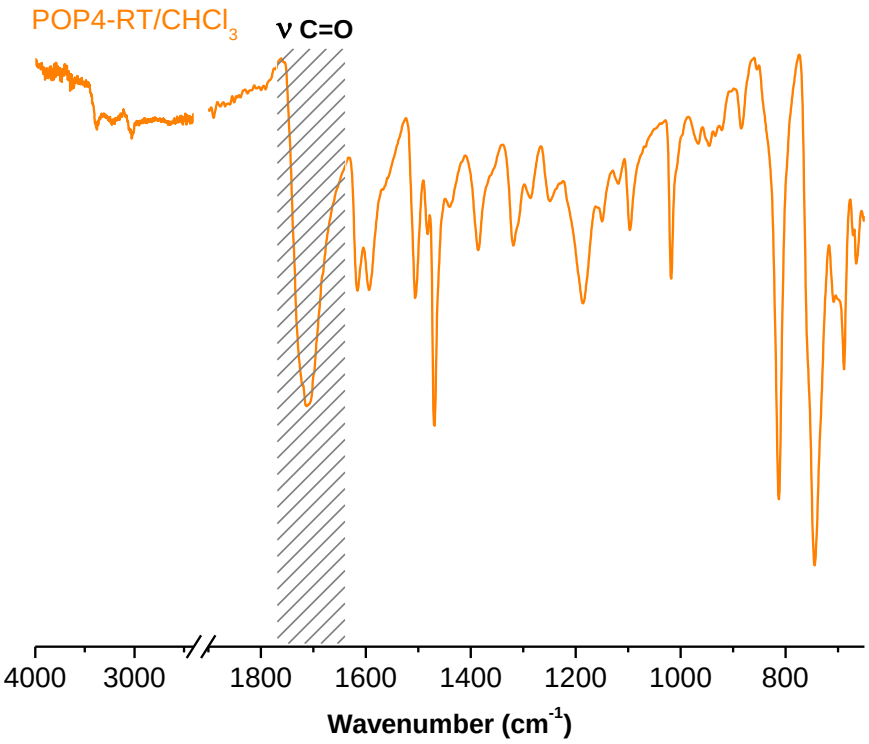

Figure S9. FTIR-ATR spectra of POP4. The dashed line region indicates the position of the C=O stretching coming from lactam ring formed during the reaction.

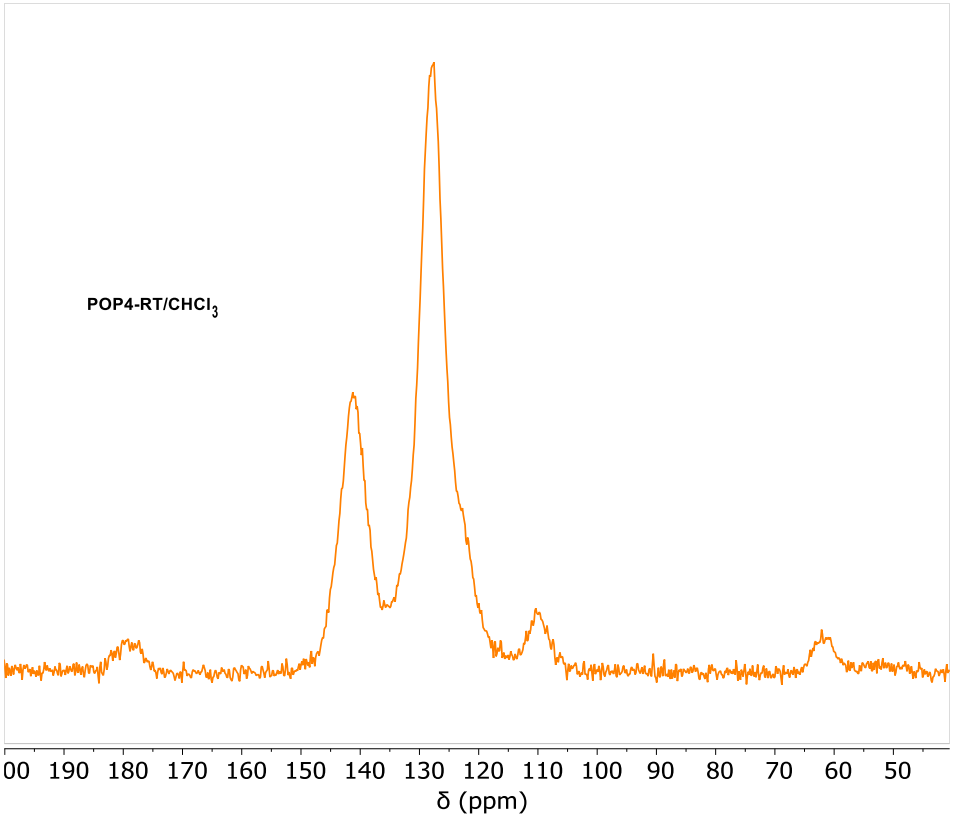

Figure S10. CP/MAS ^{13}C-NMR spectra of POP4.

Section 3. Thermogravimetric analysis of porous organic polymers

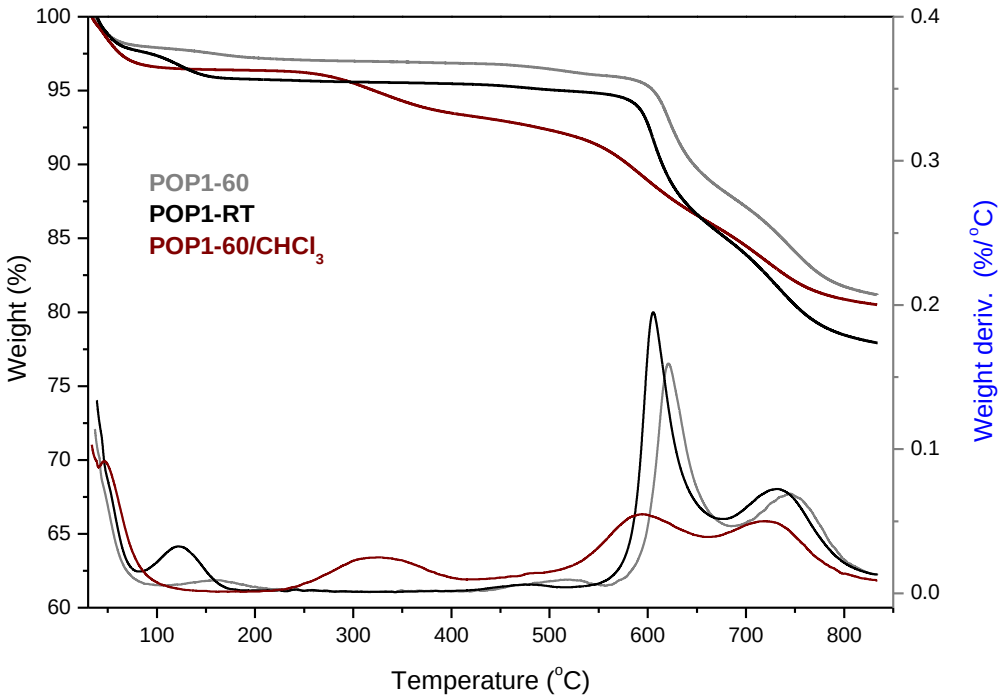

Figure S11. TGA thermograms of POP1 obtained using different reaction conditions.

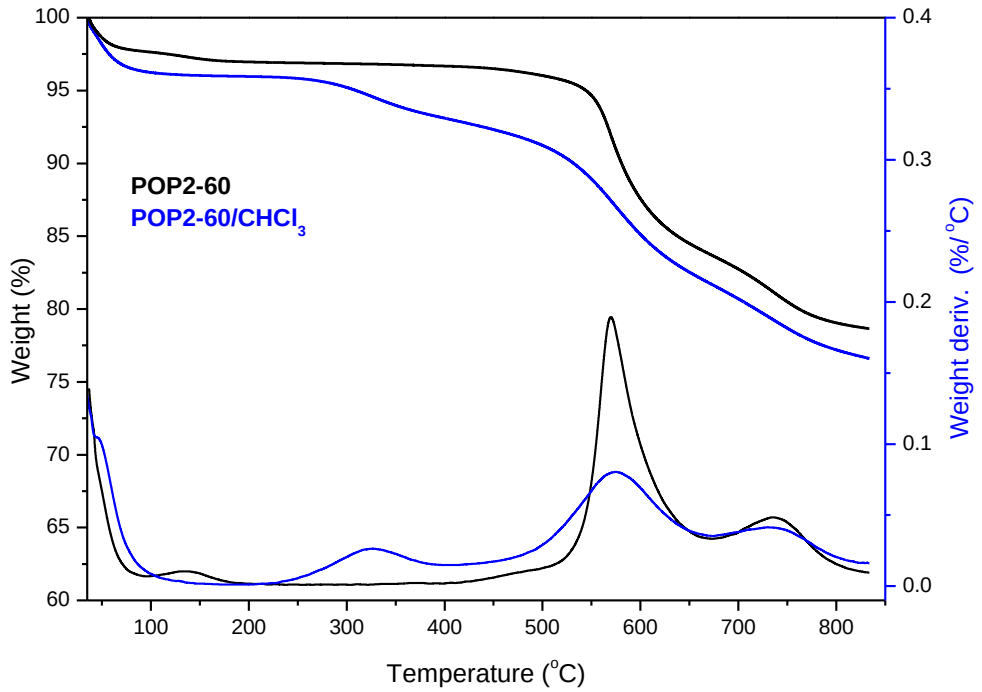

Figure S12. TGA thermograms of POP2 obtained using different reaction conditions.

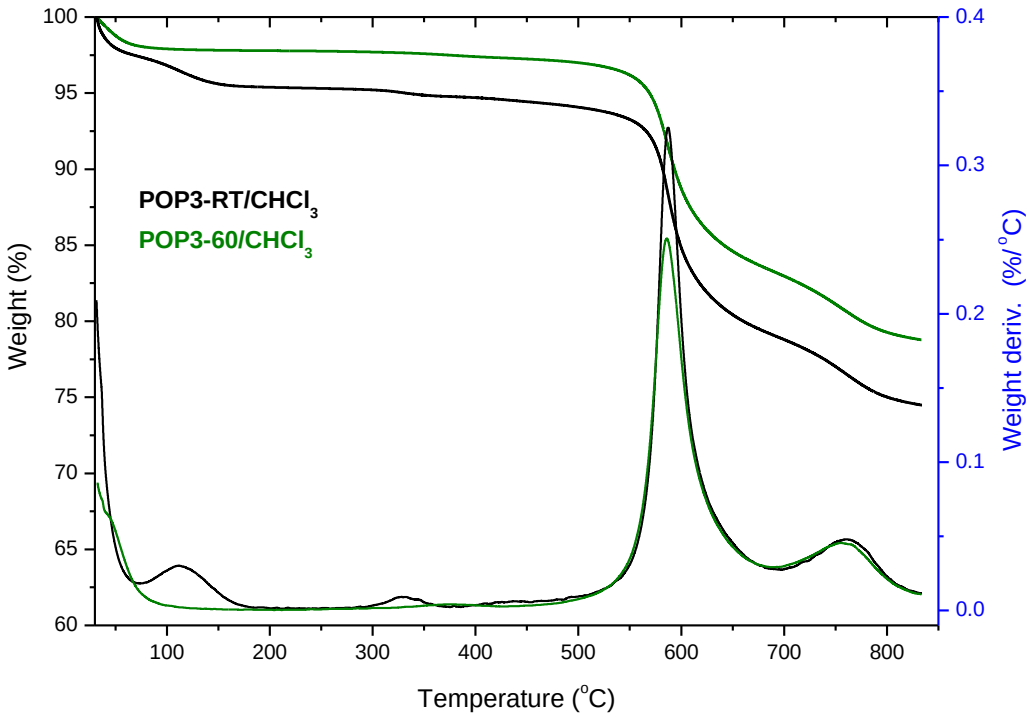

Figure S13. TGA thermograms of POP3 obtained using different reaction conditions.

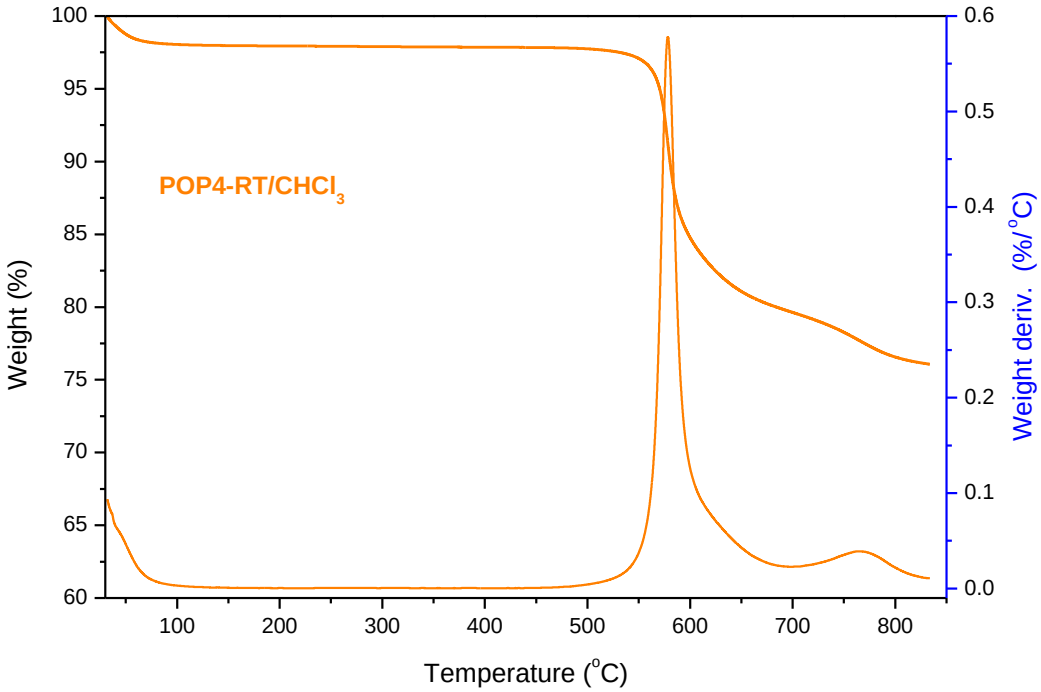

Figure S14. TGA thermogram of POP4.

Section 4. SEM and SEM-EDX characterization of Pd-supported catalysts

SEM images (250x, 15 kV) and the whole (integral) surface analysed by EDX of the samples Pd@SP-POPs.

Pd@SP-POP1

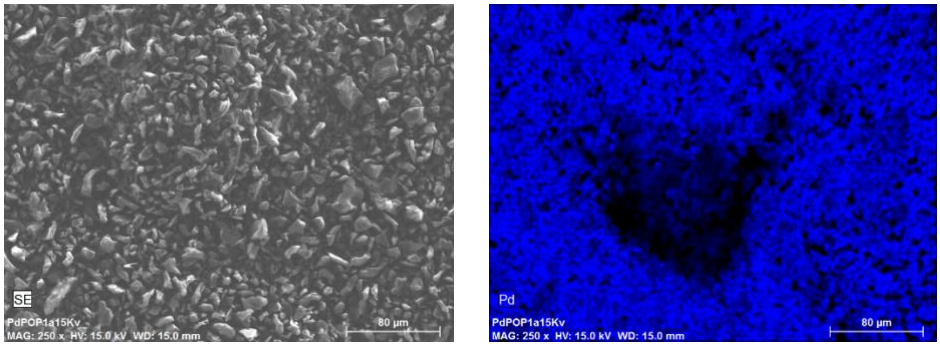

Figure S15. FE-SEM image (left) and Pd distribution (right) of Pd@SP-POP1. The error bar is of 80 µm.

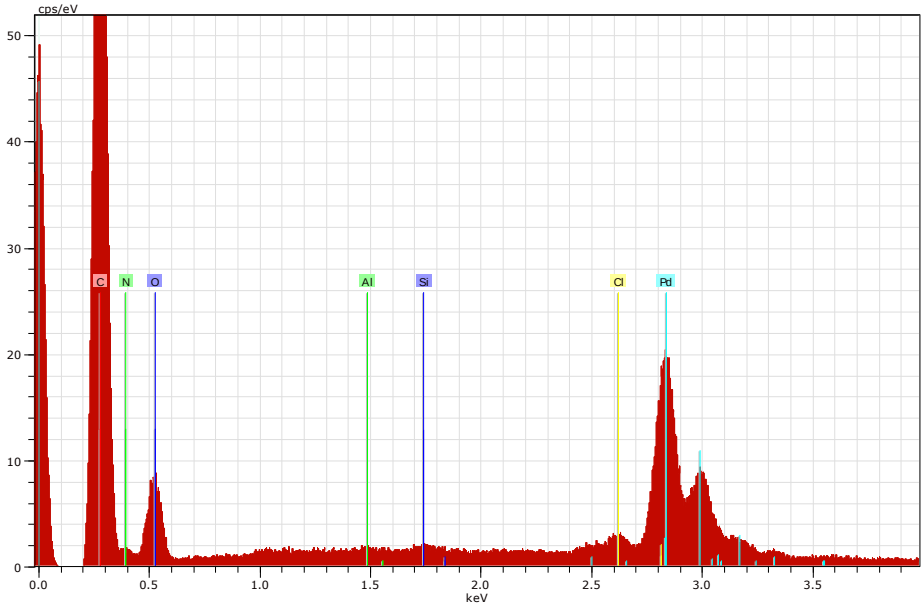

Figure S16. SEM-EDX spectrum of the surface shown in the FE-SEM image (Pd@SP-POP1**)**.

Table S2. Results of the EDX analysis of surface shown in the FE-SEM image (Pd@SP-POP1**)**

Element	Series	norm. C (wt.%)	Atom. C (wt.%)	Error (wt.%)
C	K	54.00	70.43	5.7
N	K	7.59	8.49	1.4
O	K	18.15	17.77	2.4
Al*	K	0.12	0.07	0.0
Si*	K	0.22	0.13	0.0
Cl*	K	0.61	0.27	0.0
Pd	L	19.30	2.84	0.6
	total	100.00	100.00	

*Elements (with % abundance) observed in the Pd@SP-POP1.

Pd@SP-POP2

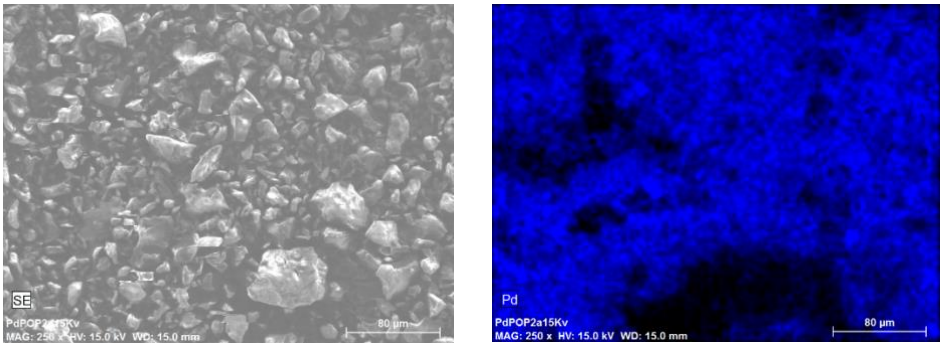

Figure S17. FE-SEM image (left) and Pd distribution (right) of Pd@SP-POP2. The error bar is of 80 μm.

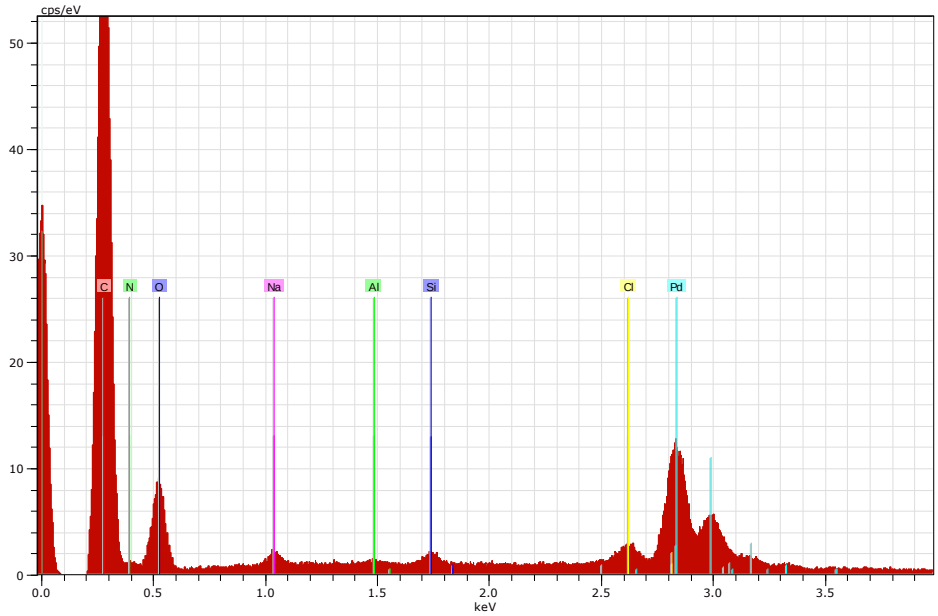

Figure S18. SEM-EDX spectrum of the surface shown in the FE-SEM image of (Pd@SP-POP2).

Table S3. Results of the EDX analysis of surface shown in the FE-SEM image of (Pd@SP-POP2)

Element	Series	norm. C (wt.%)	Atom. C (wt.%)	Error (wt.%)
C	K	54.35	70.21	6.0
N	K	5.92	6.55	1.2
O	K	20.10	19.49	2.7
Na*	K	0.63	0.43	0.1
Al*	K	0.10	0.06	0.0
Si*	K	0.51	0.28	0.1
Cl*	K	1.03	0.45	0.1
Pd	L	17.37	2.53	0.6
	total	100.00	100.00	

*Elements (with % abundance) observed in the of Pd@SP-POP2.

Pd@SP-POP3

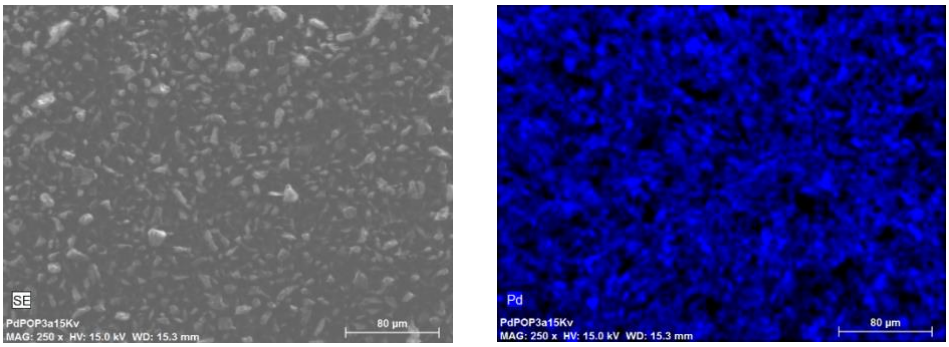

Figure S19. FE-SEM image (left) and Pd distribution (right) of Pd@SP-POP3. The error bar is of 80 µm.

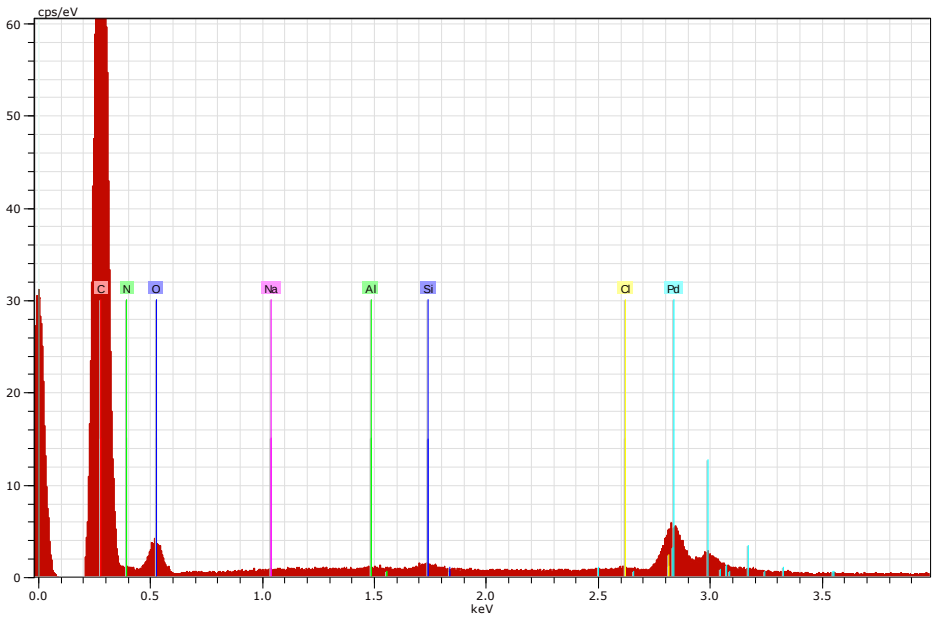

Figure S20. SEM-EDX spectrum of the surface shown in the FE-SEM image (Pd@SP-POP3).

Table S4. Results of the EDX analysis of surface shown in the FE-SEM image (Pd@SP-POP3)

Element	Series	norm. C (wt.%)	Atom. C (wt.%)	Error (wt.%)
C	K	70.97	81.14	7.9
N	K	8.56	8.39	1.7
O	K	10.49	9.00	1.6
Na*	K	0.04	0.02	0.0
Al*	K	0.07	0.03	0.0
Si*	K	0.24	0.12	0.0
Cl*	K	0.19	0.07	0.0
Pd	L	9.46	1.22	0.3
	total	100.00	100.00	

*Elements (with % abundance) observed in Pd@SP-POP3.

Section 5. Catalytic activity

Table S5. Catalytic activity comparison of Pd@SP-POPs in the Suzuki-Miyaura reaction of 4-bromoanisole with phenylboronic acid.

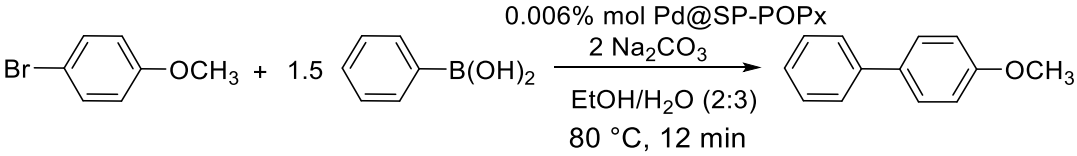

Pd@SP-POPx	Pd[a] (mg Pd/g cat)	Pd[b] (mmol)	Conversion[c] (%)	TON[d]	TOF[e] (h^{-1})
Pd@SP-POP1	172	$1.12x10^{-4}$	56	9910	49560
Pd@SP-POP2	111	$1.23x10^{-4}$	38	6180	30880
Pd@SP-POP3	64	$1.14x10^{-4}$	78	13660	68280

[a] Pd content measured by ICP-OES analysis. [b] Pd moles at 0.006% mol of catalyst, considering the catalyst weight and the metal loading determined by ICP-OES. [c] Determined by ^{1}H-NMR; [d] defined as moles of product/moles palladium ratio. [e] Defined as moles of product/(moles palladium + reaction time) ratio.

Table S6. Catalytic activity comparison of Pd@SP-POPs in the Suzuki-Miyaura reaction of 1,3-dibromo-5-*tert*-butyl-benzene with phenylboronic acid.

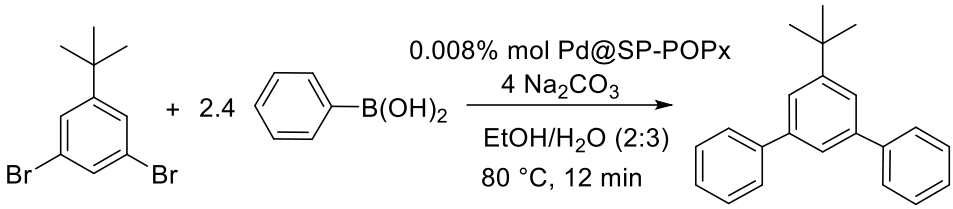

Pd@SP-POPx	Pd[a] (mg Pd/g cat)	Pd (mmol)	Conversion[d] (%)	TON[e]	TOF[f] (h^{-1})
Pd@SP-POP1	172	$1.60x10^{-4}$	4.8	597	746
Pd@SP-POP1	172	$2.78x10^{-4}$ [b]	41	2980	3730
Pd@SP-POP2	111	$1.50x10^{-4}$	0.8	ND [g]	ND [g]
Pd@SP-POP2	111	$3.70x10^{-4}$ [c]	60	3250	4060
Pd@SP-POP3	64	$1.42x10^{-4}$	30	4170	5210

[a] Pd content measured by ICP-OES analysis. [b] Pd moles at 0.014% mol of catalyst and [c] Pd moles at 0.019% mol of catalyst, considering the catalyst weight and the metal loading determined by ICP-OES. [d] Determined by ^{1}H-NMR. [e] Defined as moles of product/moles palladium ratio. [f] Defined as moles of product/(moles palladium + reaction time) ratio. [g] Not determined.

Section 6. Catalytic recycling in Suzuki-Miyaura coupling

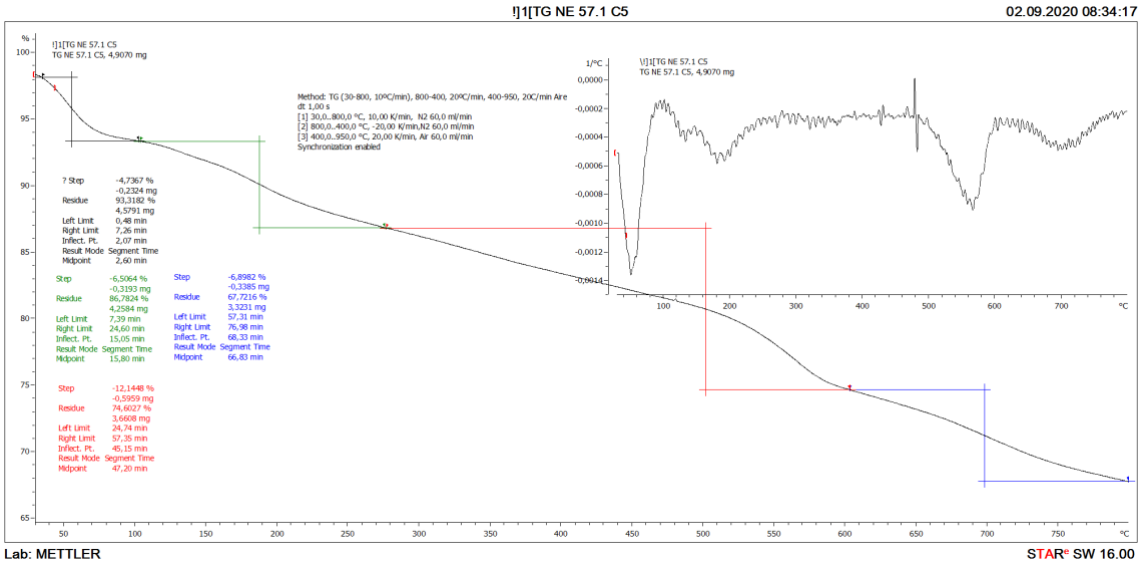

Figure S21. TGA analysis of recovered catalyst after recycling process.

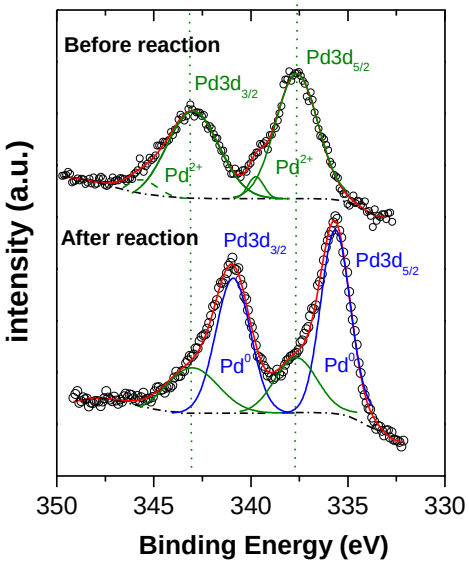

Figure S22. XPS analysis of Pd3d binding energies for Pd@SP-POP2 before and after recycling process.